Searches for Axions and for Magnetically Charged Particles Produced in e^+e^- Collisions *

NARI B. MISTRY
Floyd R. Newman Laboratory of Nuclear Studies
Cornell University
Ithaca, New York 14853

(Representing the CLEO collaboration) †

Abstract

The CLEO magnetic detector at the Cornell Electron Storage Ring *CESR* has been used to search for the production of exotic particles in electron positron collisions at center-of-mass energies around 10 GeV. We describe the search for axion-like particles in two separate experiments using radiative upsilon decays, one looking for light short-lived neutral particles decaying within the detector, the other for long-lived neutral particles escaping undetected. The search for magnetically charged particles was carried out using a novel direct method of identifying magnetic monopoles or dyons (particles carrying both magnetic and electric charge).

* Work supported in part by the National Science Foundation

† CLEO is a collaboration of the following Universities: Carnegie-Mellon, Cornell, Florida, Harvard, Ohio State, Purdue, Rochester, SUNY at Albany, Syracuse and Vanderbilt.

Introduction

Exotic particles may be produced in electron positron annihilations at high energy, for example, through a direct coupling to electrons or through the virtual photon intermediate state. The radiative decay of heavy vector mesons provides another way of producing such particles through their coupling to heavy quarks. The CLEO magnetic detector at the Cornell Electron Storage Ring *CESR* has been used to search for axion-like particles produced in the radiative decay of the upsilon (1^3S_1) state, a bound-state of the *b*- quark and its antiquark. The search for magnetically charged particles was carried out in e^+e^- annihilations over a range of energies around 10 GeV, in the region of the upsilon $^3S_1$ resonances. A novel method was used to search for pairs of magnetic monopoles by looking for pairs of trajectories with non-zero acceleration along the 1 Tesla magnetic field lines of the CLEO solenoid.

Let me begin by describing the features of the CLEO detector relevant to the two experiments. Figure 1 shows a cross-section of the detector transverse to the beam-lines at the collision point. Moving radially outward from the beam line we encounter a thin beryllium beam-pipe surrounded by a precision drift-chamber, the *vertex detector* . (During the axion search, there was multi-wire proportional chamber, with much coarser resolution.) Surrounding the vertex detector is a 17-layer cylindrical *drift-chamber* within a 1 m radius *superconducting solenoid* capable of producing a 1.5 Tesla axial field. (The 17-layer drift-chamber has recently been replaced by a 51 layer drift-chamber.) The solenoid was operated at 1 Tesla for the monopole search, but at a lower field of 0.35 Tesla during the axion search because of a concurrent search for low energy photons. *Time-of-flight* scintillators at a radius of ~2 m are used in the trigger. Note that this trigger requirement interposes about 30 g cm^{-2} of material in the path of a triggering particle.

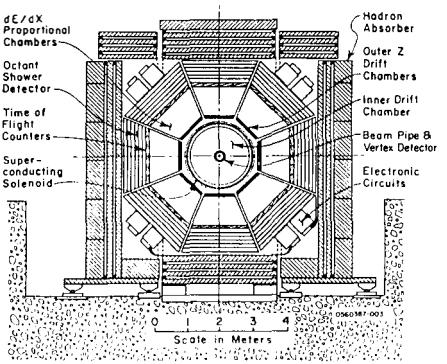

Fig. 1. Cross-section of the CLEO detector.

Axion Searches

Two axion searches were carried out in CLEO, both based on the radiative decay of heavy vector mesons

$$V_{QQ} \rightarrow \gamma + a \qquad (1)$$

where a may be any light, neutral, weakly interacting particle like an axion. Both the CUSB [1] and CLEO [2] collaborations looked for the reaction

$$e^+e^- \rightarrow \Upsilon(1S) \rightarrow \gamma + a \qquad (2)$$

where a is not detected within the active volume of the detectors and the only particle seen is a photon of beam energy. These searches were based on the assumption that axions would be very light, decaying only into $\gamma\gamma$ with a life-time longer than 10^{-9} s. The following upper limits (90% c.l.) were established:

$$\begin{aligned} &Br(\Upsilon(1S) \rightarrow \gamma a) < 3.0 \times 10^{-4} \quad \text{(CLEO)} \\ &Br(\Upsilon(1S) \rightarrow \gamma a) < 3.5 \times 10^{-4} \quad \text{(CUSB)} \\ &Br(\Upsilon(3S) \rightarrow \gamma a) < 1.2 \times 10^{-4} \quad \text{(CUSB)} \end{aligned} \qquad (3)$$

These limits, taken together with the limit [3] obtained by the Crystal-Ball experiment at SLAC for the similar radiative decay of the ψ

$$Br(\psi \rightarrow \gamma a) < 1.4 \times 10^{-5} \qquad (4)$$

can be used to rule out the standard axion[4] because in that theory *both* ($\Upsilon(1S) \rightarrow \gamma a$) and ($\psi \rightarrow \gamma a$) cannot be small.

The observation of narrow peaks in positron spectra and later in e^+e^- coincidence spectra[5] in heavy ion collisions at GSI suggested[6] the production and decay of a light neutral particle of mass about 1.8 MeV/c^2. We therefore extended our search to look for this new particle in radiative upsilon decays.[7] The decay $a \rightarrow e^+e^-$ would be observable within the one meter radius of the tracking chambers if the proper lifetime τ_0 were less than $\sim 10^{-12}$ s.

There is a problem with using the process (2) when looking for $a \rightarrow e^+e^-$, because of the large background expected from the QED process

$$e^+e^- \rightarrow \gamma\gamma \rightarrow \gamma e^+e^- \qquad (5)$$

Here the background process (5) has the same total energy as the final state being sought. To avoid this problem we look for $\Upsilon(1S)$ produced in the decay of the $\Upsilon(2S)$ resonance by observing the transition[8]

$$\Upsilon(2S) \rightarrow \pi^+\pi^-\Upsilon(1S) \qquad (6)$$

Now the background process (5) occurs at the $\Upsilon(2S)$ energy of 10,032 MeV while the signal is sought at the $\Upsilon(1S)$ energy of 9,470 MeV.

A sample of $14{,}600 \pm 500$ $\Upsilon(1S)$ decays were tagged by the transition (6) in an exposure of 22.2 pb^{-1} on the peak of the $\Upsilon(2S)$ resonance. The two tracks assumed to be pions are required to recoil against an object of mass lying within

35 MeV/c^2 of the Υ(1S) mass. Figure 2 shows an example of an event where the transition (6) is observed, with the Υ(1S) decaying into an e^+e^- pair of the right mass. Trigger and event selection cuts are more fully described in Reference 6. Candidate events should contain, in addition to a high energy photon, two low-momentum oppositely charged tracks (the pion pair) and two high-momentum oppositely charged tracks resulting from the decay $a \rightarrow e^+e^-$ in the hemisphere opposite to the photon. We allow for the possibility that the a decay into e^+e^- might produce only one rather than two distinguishable tracks because of the low mass of the pair.

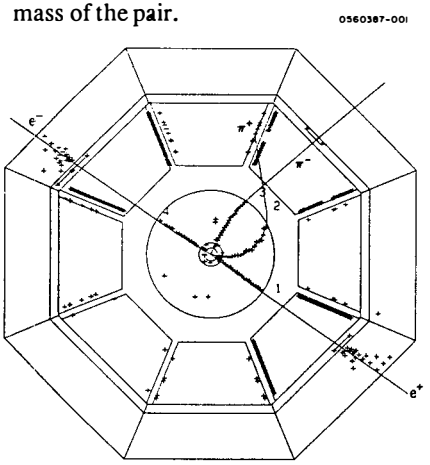

Fig. 2. An example of an event where an excited state of the Υ resonance decays into Υ(1S) by emission of $\pi^+\pi^-$ and the Υ(1S) is observed to decay into e^+e^-.

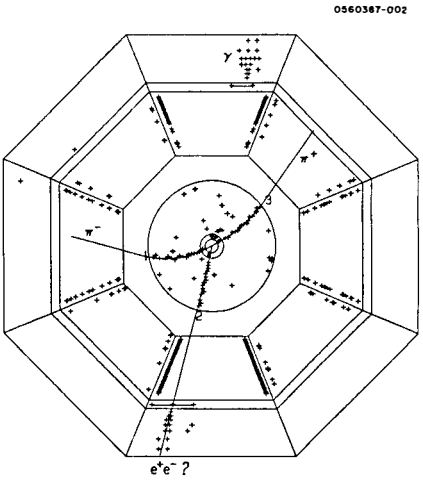

Fig. 3. One of the four candidates in the axion search. Track 2 when examined closely is incompatible with being a pair of merged tracks, and is probably an electron or positron from a converted photon.

The 21 events passing the cuts were scanned to remove events with additional unreconstructed tracks and events where a track assumed to be a pion was clearly seen to be an electron. Four candidate events remained. All four appeared to contain only single "merged" e^+e^- pairs. When examined in detail, all four of the merged pairs were inconsistent with containing two merged tracks of opposite sign, and were probably single electrons(positrons) from assymetric photon conversions. Figure 3 shows one of these four events. No candidates satisfy the criteria for acceptable events. The expected background from the decay process $\Upsilon(1S) \rightarrow e^+e^-\gamma$ was estimated to be one event.

The efficiency for detection of the decay $a \rightarrow e^+e^-$ varies with the mass m_a and the proper lifetime τ_0 of the particle a. As the lifetime of a increases it decays further from the production vertex, resulting in a decrease in the efficiency for

detection of the decay and a corresponding increase in the upper limit as a function of τ_0. This is seen in Figure 4, where we show the upper limit at 90% confidence level for the product of branching ratios $B_a = B(\Upsilon(1S) \to \gamma a) \times B(a \to e^+e^-)$ as a function of τ_0 for different masses, m_a. The previous upper limits[2] on $B(\Upsilon(1S) \to \gamma a)$, where a decays beyond the active volume of the detector, are shown also. At small lifetimes ($\tau_0 < 5 \times 10^{-13}$ s), the two results together place an upper limit of 5×10^{-4} on B_a. At large lifetimes ($\tau_0 > 3 \times 10^{-11}$ s), the limit on B_a is 3×10^{-4}. An overall upper limit of $B_a < 2 \times 10^{-3}$ applies to all lifetimes, for masses $2m_e < m_a < 2m_{\mu\mu}$.

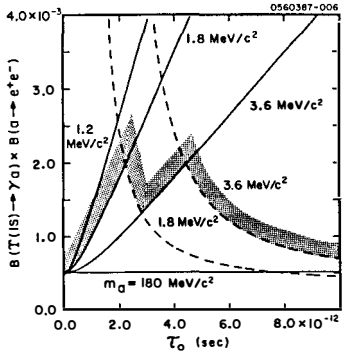

Fig. 4. Upper limits at 90% confidence level on $B_a = B(\Upsilon(1S) \to \gamma a) \times B(a \to e^+e^-)$ as a function of the proper lifetime τ_0 for observable decays of the a (solid curves) and on $B(\Upsilon(1S) \to \gamma a)$ for the previous search (Ref. 2) (broken curves).

What do these bounds have to say about the *standard axion*?[4] In this theory, the couplings of the standard axion to fermions depends on x, the ratio of the vacuum expectation values of the two Higgs fields in model. The coupling to charge $Q=2/3$ quarks is proportional to x, while the coupling to $Q=-1/3$ quarks and to charged leptons is proportional to $1/x$. The coupling can be "rotated" *up* or *down* to favor ($\psi \to \gamma a$) *or* ($\Upsilon \to \gamma a$), but *not both*! The mass and lifetime of a are also functions of x. Thus, if we choose m_a, then x and τ_0 are determined, so that $\Gamma(\Upsilon \to \gamma a)$ can be calculated. For example, if $m_a = 1.8$ MeV/c^2, then $x = 0.04$ and $\tau_0 \sim 4 \times 10^{-12}$ s. The flight path $\gamma\beta c\tau_0 = 3.2$ m and the particle would decay *outside* CLEO. The decay width $\Gamma(\Upsilon(1S) \to \gamma a) \sim 5 \cdot \Gamma(\Upsilon(1S) \to \mu\mu)$. This would lead to a branching ratio $B_a = 0.16$, enormous compared to the earlier CLEO result[2] where $B_a < 10^{-3}$. As another example, let us choose a standard axion that could be observed to decay *inside* CLEO: $\tau_0 = 3 \times 10^{-13}$ s, so that $\gamma\beta c\tau_0 = 0.13$ m, well inside the tracking volume of CLEO. This yields a mass $m_a = 3.6$ MeV/c^2 and $x = 0.02$. Thus the coupling has been turned "downwards" to favour ($\Upsilon \to \gamma a$) : we now expect an even larger rate $\Gamma(\Upsilon(1S) \to \gamma a) \sim 21 \cdot \Gamma(\Upsilon(1S) \to \mu\mu)$. The expected branching ratio product is then $B_a \sim 0.67$, which is over a thousand times larger than the upper limit observed. It would also imply that the $\Upsilon(1S)$ decays mainly into axions!

What about *non-standard* axions? Models have been proposed[9,10] that try to accomodate a large coupling to electrons to yield a short lifetime for $a \to e^+e^-$ while at the same time reducing the coupling to *both* Υ and ψ. However, each such model requires its own unpalatable peculiarities, such as flavour-changing couplings[9] or violation of e-μ universality.[10] Beam-dump experiments,[11] however, can rule out most such axions.

Search for Magnetically Charged Particles

Magnetically charged particles can be identified by their trajectory in the axial field of the CLEO solenoid. We have used this property to search for production of such particles in e^+e^- collisions up to a center-of-mass-energy of about 10.6 GeV, in the reaction

$$e^+e^- \to M\bar{M} \qquad (7)$$

where M represents either a *Dirac monopole* carrying magnetic charge g, or a *dyon* carrying both magnetic charge g and electric charge q. Note that our search[12] is limited to a range of g less than the unit Dirac charge $g_0 = (2\alpha)^{-1}e = 68.5e$ due to restrictions imposed by our trigger requirement described below.

The signature of a particle carrying magnetic charge is a trajectory indicating *acceleration along magnetic field lines.* The CLEO tracking chambers (Figure 1) are placed in an axial field of 1 Tesla, and provide 10 measurements of the z-coordinate along the beam axis as well as 27 measurements of (r,φ) coordinates. Tracks in a uniform magnetic field $|B| = B_z$ can be parametrized by $z = a_0 + a_1 s + a_2 s^2$, where s is the arc length along the trajectory in the (r,φ) plane. The quadratic fit applies to the trajectory of a magnetically charged particle experiencing a constant force along the z axis. For a particle with no magnetic charge, a better fit is obtained with a linear fit $z = a_0 + a_1 s$. In Figure 5 we show the trajectories in (s,z) of pairs of particles produced back to back, together with least-squares fits. A linear fit is best for particles with no magnetic charge, while a quadratic fit is required for the magnetically charged pair. The statistical significance of a quadratic fit is evaluated by using the F - test[13] for the improvement in χ^2 from adding the extra term to the linear fit. For magnetically charged particles we require that the χ^2 for a linear fit be large (a poor fit) and that the value of F be large (a significant improvement with a quadratic fit).

Data collected during an exposure of 25 pb^{-1} in the region of the $\Upsilon(4S)$ resonance at ~ 10.6 GeV were used for the search. An additional exposure of 159 pb^{-1} was used for a rapid search for pure monopoles ($q = 0$). The trigger demanded a hit in each of two time-of-flight (TOF) counters, requiring the particles to traverse ~ 30 g cm^{-2} of material. Selected events[12] were required to

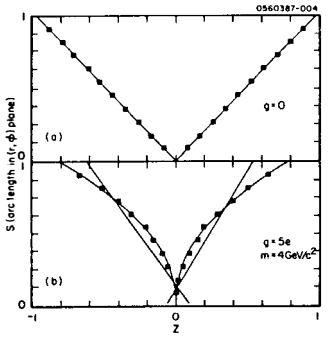

Fig. 5. Trajectories in the (s-z) plane of pairs of (a) electrically charged particles with linear least squares fits and (b) particles with magnetic charge g=8e and mass 3 GeV/c^2, shown with linear and quadratic fits.

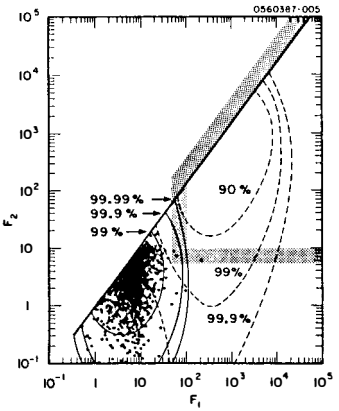

Fig. 6. Correlation plot F_1 vs. F_2 for observed events (data points). Also shown are Monte-Carlo generated contours for Bhabha events (solid) and for particles with magnetic charge g=8e and mass 3 GeV/c^2 (broken contours).

have only two tracks, each with at least six measurements of z. The fitting parameters could then be used to calculate the value of F associated with each track, such that $F_1 > F_2$. The fits of both tracks to straight lines in (s,z) were required to be poor, $\chi^2/_\nu > 12$. Events were retained if the two tracks had values of a_2 with opposite signs.

The correlation between F_1 and F_2 for the events retained is shown in Figure 6. The contour lines in Figure 6 show the distribution of events produced by a Monte Carlo simulation of the passage of magnetically charged particles (g = 8e) through the detector.[12] Also shown are contour lines for simulated Bhabha events ($e^+e^- \rightarrow e^+e^-$). On the basis of these simulations, we selected as monopole candidates those events with $F_1 > 100$ and $F_2 > 10$. No events compatible with the production of magnetically charged particles were found.

What range of g and mass have we explored? The *TOF* trigger requiring traversal of 30 g cm^{-2} limits the range to $g < 10e$, since the stopping power increases with g. In future experiments an improved detector, CLEO-II, will incorporate a trigger with minimum traversal of material, extending the range to $g \sim 70e$. The mass range is restricted by the e^+e^- collision energy of 10.6 GeV to m_M = 5 GeV.

Upper limits derived from the calculated efficiencies are shown in Figure 7 as a function of the particle mass. Curves (a, b, c) are shown for magnetic monopoles with charges g = (2e, 5e, 8e) and q = 0, from the data analysed *without*

regard to the electric charge q. Curves (f, g, h) are shown for a larger exposure of 159 pb^{-1} over a wider energy region, and analysed for events with two tracks of more than 7 GeV/c each. These "straight" tracks in the (r,φ) plane correspond to trajectories of particles with zero electric charge. No events were found at any value of F_1 , F_2 . Results from two earlier searches[14] performed at the ISR at CERN and at PEP at SLAC are also shown in Figure 7. Upper limits for *dyons* have been derived[12] using curves (a -c) and efficiencies relative to particles with $q = 0$. The limits for $q = 1$ are very similar to those shown in curves (a -c).

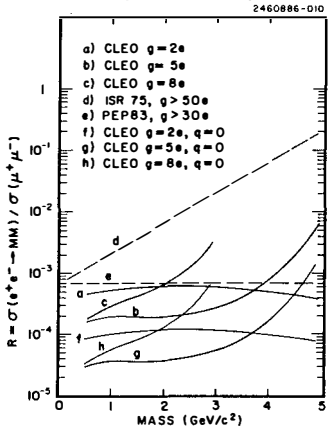

Fig. 7. Upper limits at 90% c.l. for production of monopoles. Curves (a-c) are from the data analysed without regard to electric charge, but shown for q=0. Limits for q= 1 are very similar. Curves (f,g,h) are from a search for electrically neutral particles, from a larger data set. Results from previous searches are shown as (d,e).

Conclusions

Stringent limits have been placed on the production of light, neutral, scalar particles that decay into e^+e^- pairs. These limits are orders of magnitude below predictions for the standard axion. Limits are also presented for the production in e^+e^- collisions of magnetically charged particles over a limited range of mass and magnetic charge g.

References

1. M. Sivertz *et al.*, Phys. Rev. **D26**, 727 (1982).
2. M. S. Alam *et al.*, Phys. Rev. **D27**, 1655 (1983).
3. C. Edwards *et al.*, Phys. Rev. Lett. **48**, 903 (1982).
4. S. Weinberg, Phys. Rev. Lett. **40**, 223 (1978); F. Wilczek, Phys. Rev. Lett. **56**, 2676(1986).
5. For a review see P.Kienle, Ann. Rev. Nucl. Sci. **36**, 605, 1986, and references therein.
6. A.Schäfer *et al.*, Phys. Lett. **B149**, 455(1984); A. Balantekin *et al.*, Phys. Rev. Lett. **55**, 461(1985).
7. T. Bowcock *et al.*,Phys. Rev. Lett. **56**, 2676 (1986).
8. D. Besson *et al.*, Phys. Rev. **D30**, 1433 (1984).
9. R. Peccei *et al.*, Phys. Lett. **B172**, 435 (1986).
10. L.Krauss and F. Wilczek, Phys. Lett. **B173**, 189 (1986).
11. E. M. Riordan, these *Proceedings.*
12. T. Gentile *et al.*, Phys. Rev. **D35**, 1081 (1987)
13. P. Bevington, *Data Reduction and Error Analysis for the Physical Sciences*, McGraw Hill.
14. G. Giacomelli *et al.*, Nuovo Cim. **A28**, 21(1975); D.Fryberger *et al.*, Phys. Rev. **D29**, 1524(1984).